Supporting Information

Kaiser and Warrick 10.1073/pnas.1411925111

SI Text

Cells circulate among mound layers and then among ridge layers. The repeated, periodic dispersal of cells from the fifth layer down to the fourth layer continues through the end of Movie S3 (Table 1). A similar pattern appears to continue into Movie S4 on day 5 where the entire microscopic field, all of the way to the outer edge of the swarm, is covered with long ridges that appear to have five layers. The ridge cells appear to move up and down from one layer to the next, like mound cells. There are a few isolated cells in addition to the ridges. The circulation of cells from the top layer of the ridge (which would have direct access to air) layer by layer to the bottom layer of the ridges (which would have direct access to other nutrients from the medium) would give cells equal access to oxygen and to the other nutrients. As pointed out in the Introduction, equal access allows the cells to grow at their maximum rate. If, on day 5, the cell density exceeds the level where the circulation of cells can provide enough air to support exponential growth, then the growth rate would fall and the cells move less often, as they do when beginning to starve for oxygen. Instead of mounds, dense ridges are formed.

Polysaccharide fibrils are required to build a mound. S-motility is correlated with the forceful retraction of type IV pili (1–3). In addition to pilus fibers, S-motility requires fibril polysaccharide. We hypothesize that the tips of *Myxococcus xanthus* pili attach specifically to fibril polysaccharide and that no other proteins beyond those at the base of the pilus are required for its retraction. Fibrils are found in the extracellular matrix (ECM) (4). ECM extracts contain equal amounts of protein and a repeat unit polysaccharide that contains galactose, glucosamine, glucose, rhamnose, and xylose (5–8). We hypothesize that fibrils produce elastic meshworks of strands that can bundle neighboring cells close together, as has been revealed in scanning electron microscope (SEM) images (9). Because the *dsp*/*dif* mutants, which are deficient in fibrils, can accept them from an extracellular polysaccharide fraction of normal cells (4) and regain their S-motility, we suggest that the tips of *M. xanthus* pili attach specifically to fibrils. We also suggest that pilus attachment to fibrils has the strength to withstand the full force of pilus retraction, about 100 pN, without letting go (10). The *dsp*/*dif* mutants grow dispersed in liquid culture because the mutants down-regulate fibril production. *Pseudomonas aeruginosa* PAK type IV pili, which are structurally similar to *M. xanthus* pili, have been shown to bind the polysaccharide asialo-GM1 (11), offering a precedent for a specific polysaccharide binding to type IV pili. We suggest that proper attachment of *M. xanthus* pili to fibrils specifically initiates a retraction that is strong enough and fast enough to account for the repeated explosive dispersions of Table 2. When viewed by Field emission SEM, fibrils with 30 nm or greater diameters were most often seen beyond the cell surface (6). This observation suggests that small-diameter fibrils are secreted by each cell in a cluster and that those small fibrils assemble extracellularly with other small fibrils from adjacent cells to form the 30-nm-diameter fibrils that can be observed in the SEM. As shown by the rescue experiments, fibrils persist in growing cultures as closed meshworks of cohesive and elastic polysaccharide chains whose gross structure can be modeled as in Figure S1. When pili attach to fibril strands that are bundling clusters of cells and retract, then the direction that the cell with pili moves would be determined by the spatial distribution of the clusters of cells that lie ahead and within a pilus length of the moving cell. We suggest that, once a proper attachment of the pilus tip to a fibril bundle has been made, several events unfold in sequence: The pilus retracts forcefully, the pilus-retracting cell pulls itself toward the target fibrils, and the cell associates with the fibril-bundled cluster of cells. Finally, the newly associated cell synthesizes more fibrils that bundle the now enlarged cluster. By tying several rod-shaped cells together side by side, fibrils automatically organize those cells into something like a layer of a multilayered mound. Such a sequence would account for rebuilding the fifth layer observed in Movie S5.

The loss of cells from a patch of second-layer cells on a raft resembles the loss of the entire fifth layer in an explosive dispersion. Because of the similarity, we have followed the steps taken in the slower (and unsynchronized) loss of cells from a patch. The large raft identified in Fig. 1 has three dark, irregular, nonoverlapping patches of second-layer cells that have areas of 1.6 μm^2, 4.0 μm^2, and 4.7 μm^2. Fig. S5 provides evidence that the patch areas are proportional to the number of cells each patch contains. With time, all three patches were observed to shrink. Patch 1 disappeared completely after 6 min, as shown in Fig. S2. Patch 1, patch 2, and patch 3 also shrank step-wise. Step-wise shrinking could result from the uncorrelated loss of single cells from each patch. Assuming that the patches of second layer had arisen earlier in the raft's history, we searched for earlier stages among the rafts inside the swarm edge and closer to the swarm center. There, we found several rafts with patches of second layer that were enlarging. Might the patches enlarge cell by cell following the attachment of pili from different (unsynchronized) cells to fibrils? Indeed, the following observations are consistent with addition of single cells one by one. One of the raft candidates, 0.5 min after its patch of second layer first appeared is indicated by a black arrow in the 41.0 min panel of Fig. S3. Overall, the raft is a shade of gray, and it has several fuzzy white spots indicative of gaps yet to be consolidated. At 41.0 min, the black second layer patch has an area of 0.20 μm^2. At 42.5 min, the patch enlarges further to 0.46 μm^2. At 43.5 min, the patch begins to add still more cells, finally reaching an area of 0.97 μm^2 at 44.5 min (see plot of patch area versus time in Fig. S3). The next to last cell to be added at 44.0 min can be seen to initiate a separate smaller patch slightly below and to the right of the patch indicated by the arrow in Fig. S3. Then, at 44.5 min, several cells are added joining the two patches into one large patch (black arrow). Because the patch, representing a single layer of cells, is black, we can take its area to be directly proportional to the number of cells that it contains. The complete time course of patch enlargement is presented at the right side of Fig. S3 whereas individual frames, with their time, are at the left of the figure.

Another raft, whose image is not included in Fig. S3, was found near the first, and its increase in patch area was noted. It grew cell by cell (0.126 μm^2/min) from 36.0 min until 37.5min. For that raft, we were able to estimate that an area of 0.126 μm^2 most likely represented an elongated cell that is ready to divide. This second layer enlarged to 0.5 μm^2 of cells at 37.5 min. The area and shape of the patch held steady for an additional 2 min before beginning, at 43 min, a final rise to 1.3 μm^2, estimated to be 10.3 ± 0.5 cells. These data, together with the data of Fig. S3, imply that raft second layers grow in patches of limited size. Particular regions on the top of the first layer of each raft appear to have a restricted capacity to accept second-layer cells. Cells seem to be added to each region one by one until its capacity is reached. From these observations, we infer that the capacity is the number of cells in one close-packed layer that fits inside an envelope of fibrils shown in Fig. S1.

1. Hodgkin J, Kaiser D (1977) Cell-to-cell stimulation of movement in nonmotile mutants of *Myxococcus*. *Proc Natl Acad Sci USA* 74(7):2938–2942.
2. Hartzell P, Shi W, Youdarian P (2008) *Gliding Motility of Myxococcus xanthus. Myxobacteria, Multicellularity and Differentiation*, ed Whitworth DE (ASM, Washington, DC), pp 103–132.
3. Kaiser D (1979) Social gliding is correlated with the presence of pili in Myxococcus xanthus. *Proc Natl Acad Sci USA* 76(11):5952–5956.
4. Lu A, et al. (2005) Exopolysaccharide biosynthesis genes required for social motility in Myxococcus xanthus. *Mol Microbiol* 55(1):206–220.
5. Behmlander RM, Dworkin M (1991) Extracellular fibrils and contact-mediated cell interactions in *Myxococcus xanthus*. *J Bacteriol* 173(24):7810–7820.
6. Behmlander RM, Dworkin M (1994) Biochemical and structural analyses of the extracellular matrix fibrils of *Myxococcus xanthus*. *J Bacteriol* 176(20):6295–6303.
7. Yu R, Kaiser D (2007) Gliding motility and polarized slime secretion. *Mol Microbiol* 63(2):454–467.
8. Dworkin M (1999) Fibrils as extracellular appendages of bacteria: Their role in contact-mediated cell-cell interactions in *Myxococcus xanthus*. *BioEssays* 21(7): 590–595.
9. Kearns DB, Shimkets LJ (2001) Lipid chemotaxis and signal transduction in Myxococcus xanthus. *Trends Microbiol* 9(3):126–129.
10. Maier B, et al. (2002) Single pilus motor forces exceed 100 pN. *Proc Natl Acad Sci USA* 99(25):16012–16017.
11. Giltner CL, et al. (2006) The *Pseudomonas aeruginosa* type IV pilin receptor binding domain functions as an adhesin for both biotic and abiotic surfaces. *Mol Microbiol* 59(4):1083–1096.

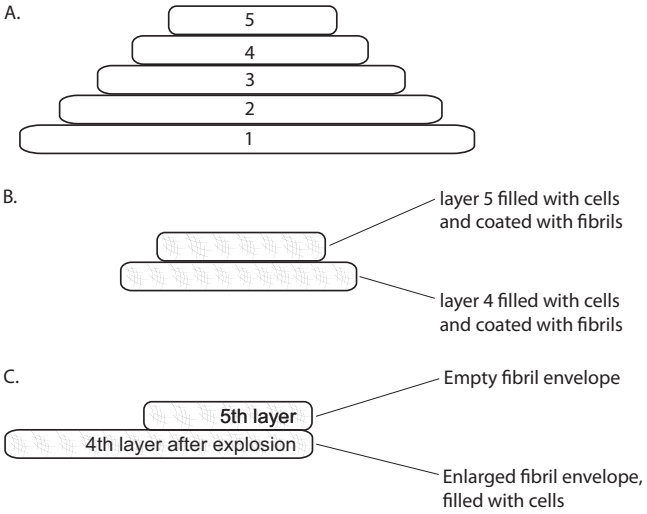

Fig. S1. Stack of five envelopes. (*A*) This diagram shows a stack of five "envelopes," each of which represents a unique network of fibrils, one that encloses and defines each layer of a mound. (*B*) Fibril networks, as a combination of a thick lined ellipse, and cross-hatched networks representing the several fibril diameters that together define each one of the envelopes. Rod-shaped cells are not visible because their view is blocked by the polysaccharide fibril envelope, as apparent in Fig. 2*B*. Only layers 4 and 5 are represented because they are sufficient to account for rebuilding a layer after an explosive dispersion of the mound. When pili attach to fibrils and they retract, as described in the *SI Text*, the cells are thought to be pulled inside an envelope. (*C*) Envelope 4 and envelope 5 just after an explosive dispersion.

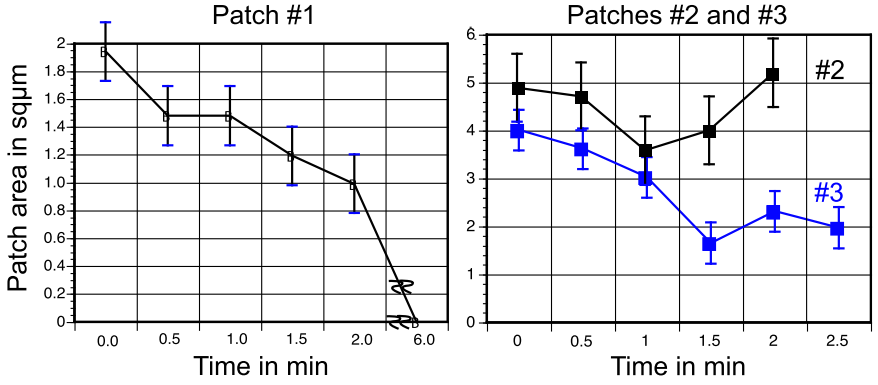

Fig. S2. (*Left*) Time course showing the loss of area from patch 1. Note the break in the horizontal scale between 2 min and 6 min. (*Right*) Time courses showing the changes of area of patch 2 and patch 3.

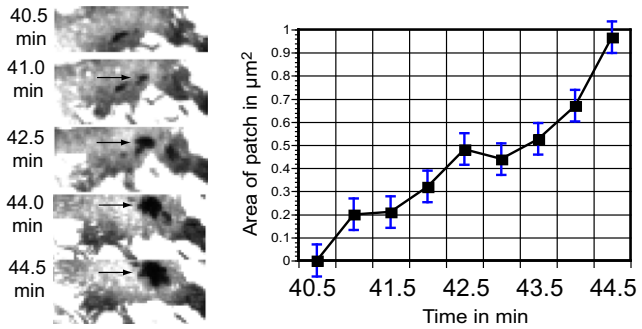

Fig. S3. (*Left*) Snapshots taken at 0.5-min intervals showing the enlargement of a patch of cells that is forming a second layer on a single layered peninsula that is projecting outward from the swarm center. Time point 40.5 min shows the peninsula before the patch is evident; 41.0 min shows the first appearance of the patch; and 42.5 min, 44.0 min, and 44.5 min show the enlargement of the patch, which is identified by an arrow. The time course of enlargement is presented at the *Right*. Error bars show the SD.

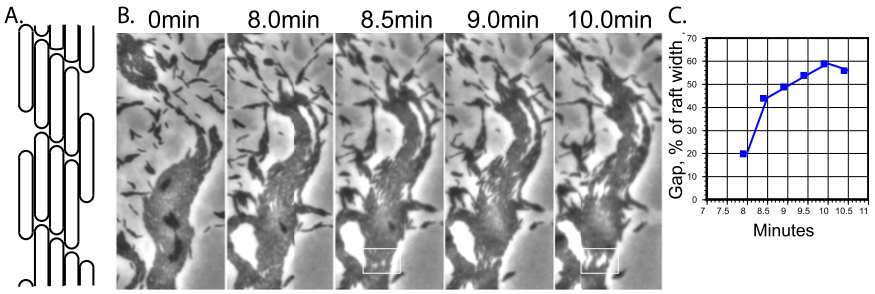

Fig. S4. Opening of cell-free gaps within a raft of cells reflects the consolidation of spaces between cell ends. (*A*) Sketch of the cell arrangement in a raft, emphasizing the long, side-by-side courses of cells whose rounded ends are out of register from one course to the next. There is more space between the ends of cells in the courses at the left and right edges of the raft than the interior courses. (*B*) From left to right are snapshots of the first movie frame (0.0 min) and the later frames at 8.0 min, 8.5 min, 9.0 min, and 10.0 min; the sequence shows the enlargement of the gap indicated by white boxes in the 8.5 min and 10.0 min panels. A kinetic curve of gap width as a function of time is presented in *C*. The width of the gap was measured along the same line enclosed by both white boxes in *B*.

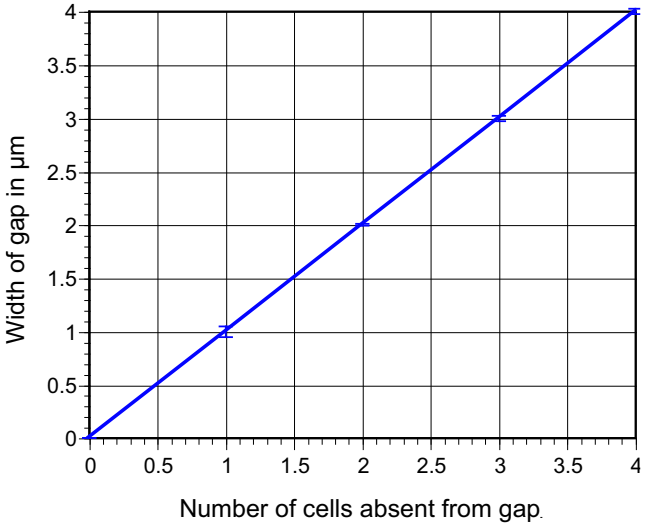

Fig. S5. The opening of gaps provides evidence that cells reverse independently and that the size of a gap is proportional to the number of cells that are missing from the gap. As shown, gaps known to be missing 1, 2, 3, or 4 cells are produced in direct proportion to the time. If reversals are not synchronized, the size of a gap should be proportional to the number of cells missing from the gap. Data points on the line are averages of 10 measurements. Error bars show the SD.

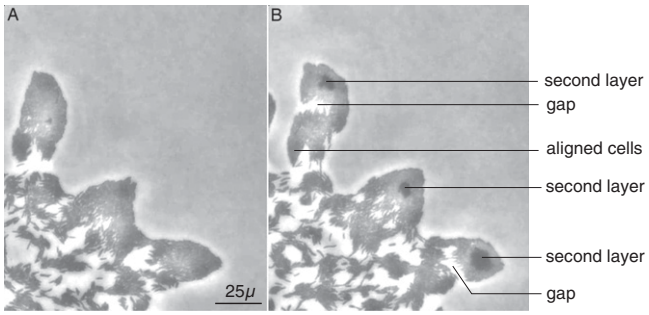

Fig. S6. Arrowheads. Cell arrangement in a streak from the edge of a swarm that lacks CglB lipoprotein. (*A*) The first frame of a movie made of that mutant. (*B*) The last frame of the movie, 1 h later.

Table S1. Repeated explosive dispersions of the mound top layer

Fifth Layer	Time of the explosion, min	Area of fifth layer before explosion, μm^2	Area added to periphery of fourth layer, μm^2
First explosion	7.0*	30.9 ± 3.53	31.18 ± 5.14
Second explosion	21 ± 1	17.3 ± 2.52	16.8 ± 2.61
Third explosion	36.7 ± 0.5	16.8 ± 2.66	9.1 ± 1.94

Number of independent measurements of the area for each sample, $n = 15$. Measured areas are tabulated in μm^2 ± SD.
*The first dispersive explosion is evident following the 7 min frame of Movie S5. The 7 min frame corresponds to 62.5 min in the complete swarm movie, which is available online as supplemental movie s1 in ref. 1.

1. Wall D, Kaiser D (1998) Alignment enhances the cell-to-cell transfer of pilus phenotype. *Proc Natl Acad Sci USA* 95(6):3054–3058.

Table S2. A-motility proteins specifically included in the focal adhesions

Protein	Location	Predicted function	Refs.
CglB	Embedded in outer membrane; exposed both sides of membrane	Binding to protein 1 in Fig. 5	(1–4)
AglT	Associated with inner membrane	Binding to next protein, Fig. 5	(5)
AglU	Periplasm	Binding to next protein, Fig. 5	(6)
AglW	Inside surface of outer membrane	Binding to next protein, Fig. 5	(5)
AglZ	Cytoplasm	Binding protein, Fig. 5	(5)
AgmK	Periplasm, crosses inner membrane	Binds to next protein in Fig. 5	(5)
AgmX	Periplasm, crosses inner membrane	Binds to next protein in Fig. 5	(5)
AgmU	Cytoplasmic side of inner membrane	Binding protein, see Fig. 5	(5)
AgmV	Unknown	Binding to next protein, Fig. 5	(5)
AgnB	Unknown	Binding to next protein, Fig. 5	(6)
AgnC	Unknown	Binding to next protein, Fig. 5	(6)
AgnK	Unknown	Binding to next protein, Fig. 5	(6)
Mx4864*	Unknown	Binding to next protein, Fig. 5	(5)
Mx4868*	Unknown	Binding to next protein, Fig. 5	(5)
Pgl I	Associated with inner membrane	Binding to next protein, Fig. 5	(6)

Proteins listed in this table are located in different cellular compartments. CglB, for example, is a lipoprotein embedded in the outer surface of the cell's outer membrane. Each of these proteins binds to another protein also listed in this table and is numbered sequentially in Fig. 5. Signaling is proposed to be initiated by the formation of a junction between the CglB proteins in the outer membrane of two cells that come into physical contact with each other as indicated in Fig. 5. That contact induces protein 1 (Cgl B) and protein 2 (there are several candidates: Agl U, Agm K, Agm V, and is called protein 2) located in the periplasm to bind each other. The 1•2 binding then induces 2•3 binding in the next compartment, etc. Arrows in Fig. 5 point toward the next pair of A-motility proteins to bind together. In general, the number indicates the position in the sequence of pairwise binding steps unless, like CglB and FrzCD, their location is established and they are named. Designation 1•2 is the first pair of proteins to bind, 2•3 is the second pair, and n•n+1 is the next to last pair. The last pair is n+1•FrzCD although FrzCD is a methylated regulatory protein and not an A-motility protein. Once the signal has reached FrzCD in the cytoplasm of both cells, the phases of their oscillations are reset to the average value of the phase they had before this connection. Each pair of cells shown are joined for a short time: less than a minute. After the two phases are averaged, the cells disjoin and move on to pair with other cells, to spread the signal to other cells nearby.
*Shorthand for MXAN_4864 and MXAN_4868.

1. Hodgkin J, Kaiser D (1977) Cell-to-cell stimulation of movement in nonmotile mutants of *Myxococcus*. *Proc Natl Acad Sci USA* 74(7):2938–2942.
2. Nudleman E, Wall D, Kaiser D (2005) Cell-to-cell transfer of bacterial outer membrane lipoproteins. *Science* 309(5731):125–127.
3. Wall D, Kaiser D (1998) Alignment enhances the cell-to-cell transfer of pilus phenotype. *Proc Natl Acad Sci USA* 95(6):3054–3058.
4. Wei X, Pathak DT, Wall D (2011) Heterologous protein transfer within structured myxobacteria biofilms. *Mol Microbiol* 81(2):315–326.
5. Nan B, Mauriello EM, Sun I-H, Wong A, Zusman DR (2010) A multi-protein complex from *Myxococcus xanthus* required for bacterial gliding motility. *Mol Microbiol* 76(6):1539–1554.
6. Yu R, Kaiser D (2007) Gliding motility and polarized slime secretion. *Mol Microbiol* 63(2):454–467.

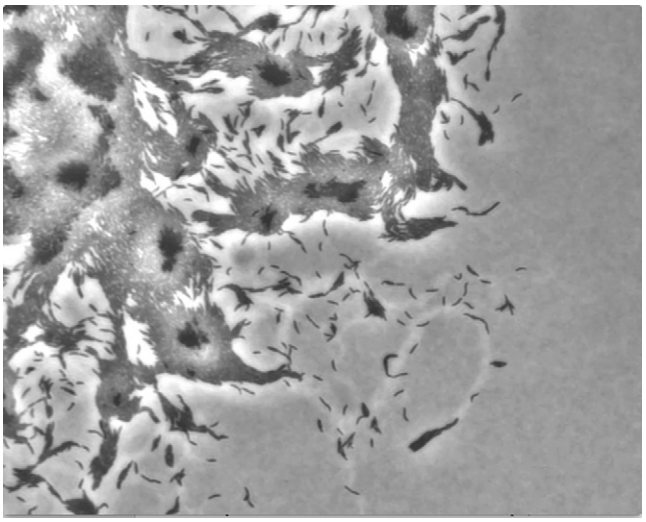

Movie S1. Swarm edge on day 1.

Movie S1

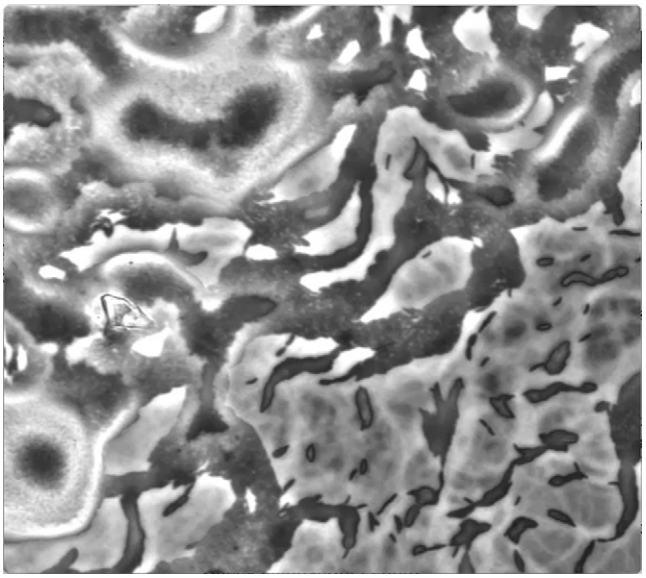

Movie S2. Swarm edge on day 2.

Movie S2

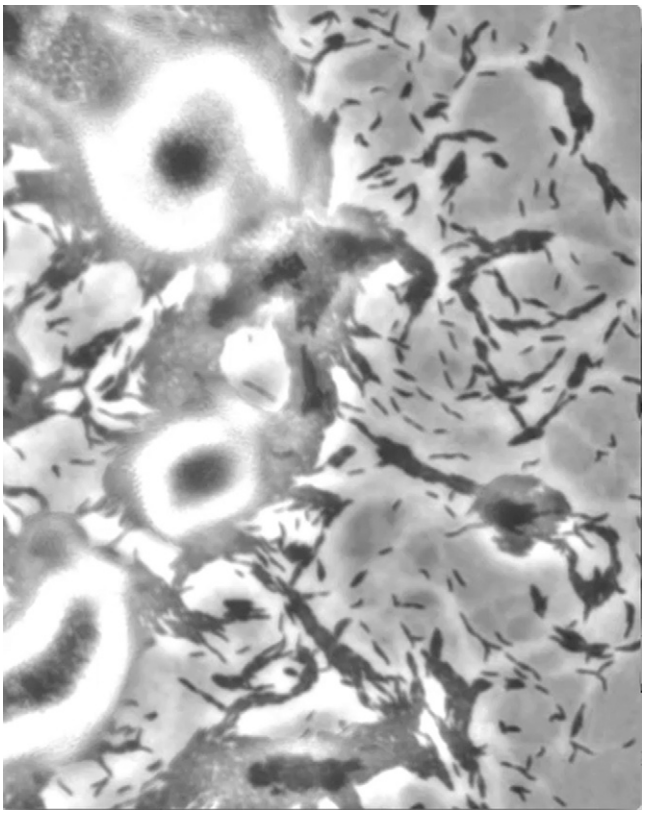

Movie S3. Swarm edge on day 4.

Movie S3

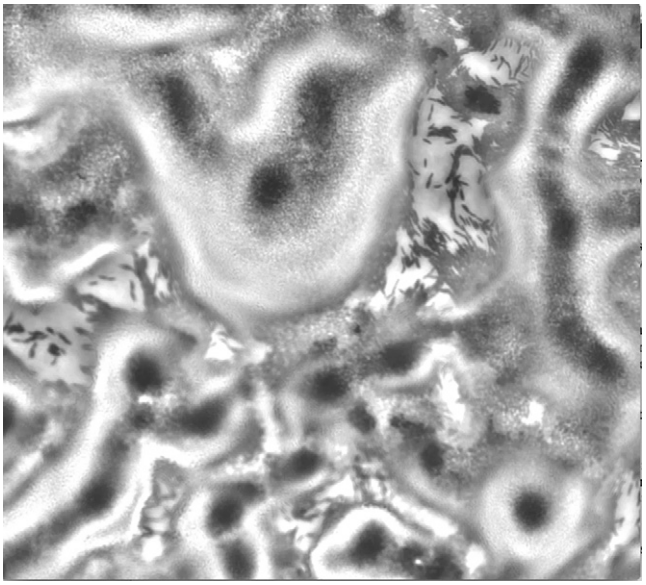

Movie S4. Swarm edge on day 5.

Movie S4

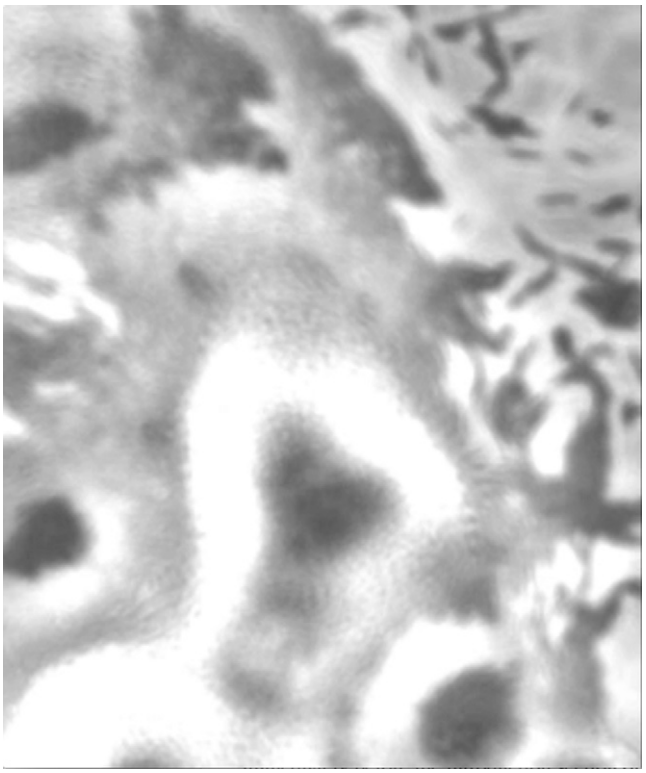

Movie S5. Three sequential explosions and reconstructions of a mound.

Movie S5